Research Square

Preprints are preliminary reports that have not undergone peer review.
They should not be considered conclusive, used to inform clinical practice,
or referenced by the media as validated information.

Non-Uniform Elastic Torsional Analysis:A Rigorous Validation of 7-Dof Warping Elements

Tugrul Talaslioglu

ttalaslioglu@osmaniye.edu.tr

Osmaniye Korkut Ata University

Research Article

Keywords: Non-uniform torsion, Vlasov theory, OpenSeesPy, 7-DOF beam element, Analytical validation, Bi-moment kinematics

Posted Date: July 13th, 2026

DOI: https://doi.org/10.21203/rs.3.rs-10314499/v1

License: This work is licensed under a Creative Commons Attribution 4.0 International License.
Read Full License

Additional Declarations: No competing interests reported.

NON-UNIFORM ELASTIC TORSIONAL ANALYSIS: A RIGOROUS VALIDATION OF 7-DOF WARPING ELEMENTS

Talaslioglu Tugrul

Osmaniye Korkut Ata Unv., Eng. And Natura Sciences Fac., Civil Engineering Dep., Fakiusagi, Osmaniye Turkiye
ttalaslioglu@osmnaniye.edu.tr , Orcid No: 0000-0002-8075-4130

Abstract

Torsion is a critical structural demand in thin-walled steel systems, where restricted warping induces complex non-uniform torsional kinematics and longitudinal normal stresses. While Vlasov's theory mathematically governs these sectorial-based mechanics, its transition into 7-degree-of-freedom (7-DOF) finite element formulations often remains obscured within the "black-box" environments of commercial software. This opacity limits structural engineers' ability to intuitively understand and accurately validate warping-induced behaviors. To address this gap, this study proposes a rigorous analytical framework and a dedicated MATLAB solver designed to transparently compute and benchmark Vlasov's fourth-order differential equations. Consequently, the perfect correlation between the two independent platforms not only validates the analytical solver as a robust theoretical baseline but also confirms the accuracy of the open-source numerical element named "elasticBeamColumnWarping" in capturing complex bi-moment distributions. Ultimately, this study provides researchers and practicing engineers with a transparent, verifiable framework for the advanced analysis of non-uniform elastic torsion.

Keywords**, Non-uniform torsion; Vlasov theory; OpenSeesPy; 7-DOF beam element; Analytical validation; Bi-moment kinematics**

1. Introduction

The structural efficiency of thin-walled steel members is frequently exploited in modern civil engineering due to their high strength-to-weight ratio. However, their open cross-sectional nature renders them highly susceptible to the torsional effects. In conventional structural analysis, the torsion is often treated using St. Venant's theory [1], which assumes that cross-sections remain plane and free to warp. St. Venant's formulation is based on the assumption of "uniform torsion," where the rate of twist is constant along the beam's axis. Under this assumption, the cross-sections of a beam undergo out-of-plane displacements, known as warping, but are considered "free". Consequently, St. Venant's theory assumes that no longitudinal normal stresses are generated due to torsion, and the torque is resisted solely by circulating shear stresses. This approach remains highly accurate for solid or thick-walled closed sections.

However, for thin-walled open sections frequently used in steel structures, St. Venant's theory becomes insufficient. The transition from uniform to non-uniform torsion occurs when warping is hindered—either by boundary conditions (e.g., fixed supports) or by variations in the applied torque along the span. This restriction of warping introduces "longitudinal normal stresses" and additional "warping shear stresses". The mathematical governance of this phenomenon was established by Vasily Z. Vlasov [2]. This is the seminal work that defined the kinematics of thin-walled sections. Vlasov established the equilibrium equations and the concept of the "shear center," proving that for open sections, warping rigidity often dominates over St. Venant rigidity [2]. Vlasov's theory of thin-walled beams introduced the concept of "sectorial-based computation method", which acts as a fundamental basis for calculating warping-induced effects, because it is the natural coordinate system of a thin-walled sections. Unlike the classical Euler-Bernoulli or Timoshenko theories, Vlasov's governing differential equation for torsion is of the fourth order. In fact, this step causes to emerge 7th DOF at each node [3].

Before Vlasov's work became widely translated, it is noted that Benscoter provided an alternative approach to non-uniform torsion, particularly focusing on how warping is distributed across the section. His work laid the groundwork for the numerical integration of warping in early finite element methods [4].

Particularly, the first details in calculating torsional constants for various industrial steel sections and translating complex theoretical derivations into practical engineering applications was handled by Kollbrunner and Basler [5]. Kollbrunner and Basler [5] provided comprehensive tables for the solutions of this fourth-order equation under various boundary conditions, simplifying the task for practicing engineers. They emphasized that for open sections, the torsional rigidity term often dominates the torsional response, especially near supports.

Bažant and El Nimeiri [6] were among the first to translate this fourth-order governance into a finite element framework. Their work highlighted that standard 6-DOF beam elements fail to satisfy the boundary conditions required by Vlasov's theory. It was laid down that the derivative of twisting angle was required for the introduction of the 7th degree of freedom (warping).

Yoo and Lee [7] demonstrated that the fourth-order nature of the equation allows for the capture of "boundary layer" effects—where warping stresses decay rapidly away from the point of restraint.

Gjelsvik [8] refined Vlasov's assumptions and provided a more rigorous mechanical derivation. This work is crucial for understanding the interaction between axial forces and non-uniform torsion, which is a cornerstone of modern steel design codes.

Trahair [9] extended the Vlasov theory to the stability of steel structures. He demonstrated that ignoring warping restraints leads to a significant underestimation of the lateral-torsional buckling capacity of beams, which is vital for the safety of steel structural systems.

The transition from Vlasov's analytical fourth-order differential equations to the Finite Element Method (FEM) represents a major milestone in structural mechanics, as it allowed for the analysis of complex, multi-span systems that were previously unsolvable by hand. The integration of warping into FEM was driven by the necessity to satisfy the boundary conditions of Vlasov's theory at the element level—specifically the requirement to enforce or release the first derivative of the twist angle, which represents the warping deformation. In a standard 3D beam element, the torsional response is governed by a second-order equation, however, Vlasov's fourth-order governance both the twist angle and the rate of twist angle (derivative of twist angle) must be continuous across element nodes. Early researchers focused on developing Hermitian shape functions to interpolate the torsional rotation, similar to those used for transverse displacements in Euler-Bernoulli beams. they were among the first to develop a finite element capable of capturing warping. Barsoum and Gallagher [10] introduced the 7th DOF at each node.

Mohri and et. al. [11] provided the theoretical basis for elements that can undergo large rotations while maintaining the accuracy of the warping restraint effects.

The recent studies have demonstrated that utilizing 7-DOF beam elements—which introduce the derivative of the twist angle as an active nodal degree of freedom—provides a highly efficient alternative to computationally expensive solid element models for capturing non-uniform torsional stresses [12-14].

The integration of non-uniform torsion into global structural analysis has historically been a challenge due to the disconnect between complex analytical formulations and user-friendly numerical tools. However, the traditional commercial finite element software often operates as a "black box," where the internal handling of the 7th degree of freedom (warping) and its interaction with other axial and flexural demands is not fully transparent. At this point, due to the need for a deeper understanding of the theoretical background within the 'black box,' open-source software has become invaluable to the scientific community Although there exist a number of open-source oded software, OpenSees [15], which is an open-source computational platform that has revolutionized earthquake and structural engineering research, provides a unique advantage by its being open for peer review and continuous refinement by the global academic community and its flexibility of being implementation for one of the most updated platforms, phyton (OpenSeesPy) [16].

In this framework, the primary objective of this study is to provide a rigorous numerical validation of the "elasticBeamColumnWarping" element utilized in OpenSeesPy. Despite its widespread use, direct benchmarking revealing its basic computing fundamentals in detail against a pure analytical Vlasov solution is sparse in current literature. By developing a dedicated MATLAB analytical solver, this work aims to actually simplify the mathematical complexity arisen form transforming the abstract fourth-order differential equations of Vlasov theory into a tangible and verifiable one. Furthermore, the validation of dedicated MATLAB analytical solver is controlled by solving a simple structural performing test which constructed by the ready profiles with symmetric, semi-symmetric, asymmetric cross-sections. It should be explicitly noted that this study strictly limits its scope to the behavior of a single element; the structural behavior of frame systems is intentionally excluded. The compelling justification is that transferring seventh-degree warping kinematics (i.e., bi-moments and warping deformations) across multi-element nodes requires highly complex, joint-specific boundary assumptions. Introducing such joint interactions would inevitably obscure the pure mathematical benchmarking of the element's core formulation, thereby preventing a transparent validation of its foundational accuracy.

Thus, the first sub-section is reserved for the introduction. Then, the methodology section which contains the mathematical basis of both St. Venant&Vlasov theories and "elasticBeamColumnWarping" element utilized in OpenSeesPy is given as second sub section. In the application section, a typical cantilever beam with Symmetric, Semi-symmetric and Asymmetric type cross-sections is considered. A discussion of results obtained from the application is also presented in this sub-section. The last sub-section is concluded with a summarization of discussed results.

2. Methodology

2.1. Motivation

The structural behavior of thin-walled open sections is governed by the interaction of Saint-Venant torsion and warping torsion [3]. Unlike Euler-Bernoulli beam theory, Vlasov's theory introduces a fourth-order differential equation to account for the resistance to warping. To solve this effectively, researchers frequently employ a mechanical analogy, most notably the "beam on elastic foundation" analogy ("Winkler hypothesis"). The primary reason for utilizing an analogy is the mathematical isomorphism between the governing equations of different physical systems. By mapping the warping torsion problem onto the well-understood behavior of a beam resting on an elastic (Winkler) foundation, engineers can leverage existing closed-form solutions and intuitive structural models (such as bending moments, flexural rigidity representing bi-moments, warping rigidity) to predict complex torsional deformations. Vlasov explicitly highlights that this equation is mathematically identical (isomorphic) to the equation of a beam on an elastic foundation subjected to axial force and lateral load. Also, Vlasov explains that the term Saint-Venant rigidity *GJ* acts like a "restoring force" or a "distributed spring support". This allows the designer to visualize the warping of the section as the bending of a beam where the "foundation" is provided by the torsional shear resistance of the material itself.

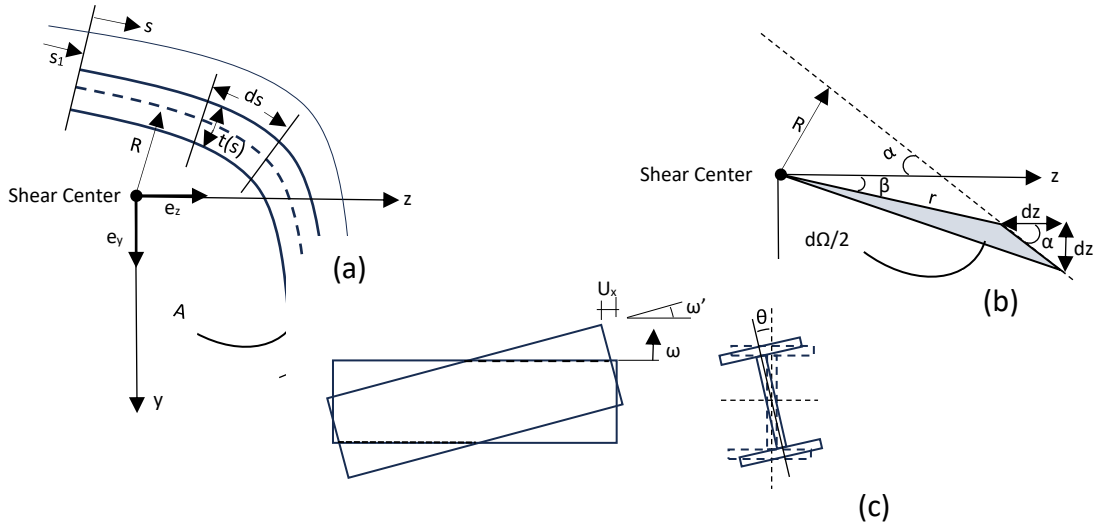


Figure 1. Sectorial-based Sketch of Warped Torsional Effects on the Cross-sections (a) and (b) and Visualization of Warped Torsional Rotational Angle and Displacement (c)

The primary limitation of classical Euler-Bernoulli also including Timoshenko theories lies in their assumption that cross-sections remain rigid in their own plane and undergo only minor out-of-plane displacements that do not affect the internal equilibrium of the beam under torsion [17]. However, the thin-walled open sections undergo significant warping (longitudinal displacement) Ux when twisted (see Figure 1). Vlasov needed a way to measure this displacement at every point along the profile. He discovered that the longitudinal displacement is directly proportional to the area "swept" by a ray originating from the rotation center. This "swept area" is computed by "Sectorial Area" Ω depending on "Sectorial Coordinates" ω and "Natural Coordinate" s unlike the Cartesian coordinates x, y and z. Furthermore, when warping is restrained, the longitudinal fibers of the beam unlike solid sections are stretched or compressed. This creates a system of longitudinal normal stresses due to only warping moment. In order to take into account of two equal and opposite bending moments acting in parallel planes, or more simply, as a "generalized torque" that specifically accounts for the resistance to warping, Vlasov also defined "Bi-moment concept".

2.2. Mathematical Fundamentals of Vlasov Theory

This section is pivotal as it defines the mathematical transition from classical beam theories to the specific kinematics of thin-walled members. The primary limitation of classical Euler-Bernoulli and Timoshenko theories lies in their assumption that cross-sections remain rigid in their own plane and undergo only minor out-of-plane displacements that do not affect the internal equilibrium of the beam under torsion. Vlasov challenged this by introducing Sectorial area Ω, often referred in Sectorial Coordinates ω. Unlike the Cartesian coordinates x, y and

z, the Sectorial area Ω is a geometric property representing the swept area from the shear center to any point on the profile's midline ($\int_A \omega dA = 0; \quad \int_A x\,\omega dA = 0; \quad \int_A y\,\omega dA = 0$)

Assuming "torsional angle" $\theta(x)$, "warping displacement" $u_x(x, y, z)$ out of the cross-sectional plane along the x-axis, the displacements in Cartesian Coordinates [14],

$$u_y(x,y,z) \equiv u_y(x,z) = -\theta(x)z \tag{1}$$

$$u_z(x,y,z) \equiv u_z(x,y) = \theta(x)y \tag{2}$$

The St. Venant (or uniform) torsion is defined by a free warping due to torsion. The strain (ϵ_x, ϵ_y, ϵ_z) and stress (σ_x, σ_y, σ_z) values in x, y and z axes are equals to zero "0".

The Vlassov (or non-uniform) torsion is defined by vanishing shear strains:

$$\left.\begin{aligned} \epsilon_x &= \frac{\partial u_x}{\partial x} \\ \gamma_{xy} = \frac{\partial u_x}{\partial y} + \frac{\partial u_y}{\partial x} &= \frac{\partial u_x}{\partial y} - \theta' z, \qquad \theta' = d\theta/dx \\ \gamma_{xz} = \frac{\partial u_x}{\partial z} + \frac{\partial u_z}{\partial x} &= \frac{\partial u_x}{\partial z} + \theta' y \end{aligned}\right\} \tag{3}$$

If the coordinates y and z are parametrized in terms of "natural coordinate" s, it is represented as $y(s)$, $z(s)$. A natural coordinate s is introduced along the thin-wall of the cross-section with thickness $t(s)$, the cross-sectional area A.

$$A = \int_{s_1}^{s_2} t(s)ds \tag{4}$$

The rate of change of longitudinal displacement along the midline of the cross-section u_x in "natural coordinate" s is,

$$\frac{du_x}{ds} = \frac{\partial u_x}{\partial y}\frac{dy}{ds} + \frac{\partial u_x}{\partial z}\frac{dz}{ds} = \theta'\left(z\frac{dy}{ds} - y\frac{dz}{ds}\right) \tag{5}$$

The perpendicular distance from the shear center R is defined as "Sectorial Radius",

$$R = r\cos(90° + \beta - \alpha) = -r\sin(\beta - \alpha) = -r(\sin\beta\cos\alpha - \cos\beta\sin\alpha) = -\left(z\frac{dy}{ds} - y\frac{dz}{ds}\right) \tag{6}$$

Thus, Eq. 5 is represented as:

$$\frac{du_x}{ds} = -\theta' R(s) \tag{7}$$

In fact, the Sectorial Radius R is also utilized in the definition of "swept area.", that is, "Sectorial Area" Ω_s. The swept area of the sector formed by the shear center, the starting point s_1 and the current point s. From this perspective, the differential area $d\Omega_s$ in Figure 1 is obtained by the vector cross-product:

$$d\Omega = |x \times dx| \tag{8}$$

The expansion form of Eq.8 is,

$$|\boldsymbol{x} \times \boldsymbol{dx}| = \begin{vmatrix} \boldsymbol{e_x} & \boldsymbol{e_y} & \boldsymbol{e_z} \\ 0 & y & z \\ 0 & dy & dz \end{vmatrix} \tag{9}$$

$$x \times dx = e_x(y \cdot dz - z \cdot dy) \tag{10}$$

$$\mathrm{d}\Omega = \mathrm{y\,dz} - \mathrm{z\,dy} \tag{11}$$

$$d\Omega = y\left(\frac{\partial z}{\partial s}ds\right) - z\left(\frac{\partial y}{\partial s}ds\right) = \left(y\frac{\partial z}{\partial s} - z\frac{\partial y}{\partial s}\right)ds = \underbrace{-\left(z\frac{\partial y}{\partial s} - y\frac{\partial z}{\partial s}\right)}_{R(s)}ds \quad (13)$$

Thus, Eq.13 is,

$$\frac{d\Omega}{ds} = R(s) \Rightarrow \Omega(s) = \int_{s_1}^{s} R(s)ds \quad \text{with} \quad \Omega(s_1) = 0 \quad (14)$$

The warping displacement u_x in Eq.7 is obtained by an integration computation depending on Sectorial Radius R and Sectorial Area Ω_s. The displacement u_x at the starting point (origin) of the contour integration s_1 is

$$u_x(x,s) = u_x(x,s_1) - \theta'\Omega(s) \quad (15)$$

If a specific point s_0 on the cross-section's midline where the longitudinal displacement due to warping is assumed to be zero, that is, $u_x(x, s_1) = 0$, Eq.15 is

$$u_x(x,s_2) = \theta'\Omega(s_1) \quad (16)$$

If Eq.16 is placed into Eq.15,

$$u_x(x,s) = -\theta'\big(\Omega(s) - \Omega(s_1)\big) = -\theta'\omega(s) \quad (17)$$

Eq. 17 defines the longitudinal displacement at the contour origin u_x. This ”normalization process” allows the sectorial area $\Omega(s)$ to be transformed into “sectorial coordinate” $\omega(s)$ with respect to the shear center effectively shifting the warping distribution to its physical null point s_0. Thus, the "relative" sectorial area measured from your reference point s_1 is utilized to define he geometric distribution of longitudinal displacement across the cross-section due to a unit rate of twist. The sectorial coordinate $\omega(s)$ is solely,

$$\omega(s) = \Omega(s) - \Omega(s_1) \quad (18)$$

The differential case of sectorial coordinate $\omega(s)$ considering definition of swept area in Figure 1 is,

$$d\omega = 2 \cdot (\text{area of triangle}) = 2.\frac{1}{2} \cdot \underbrace{ds}_{\text{base}} \cdot \underbrace{R(s)}_{\text{height}} = R(s)ds = d\Omega \quad (19)$$

The differential sectorial area $d\Omega$ is defined as twice the triangular area swept by the position vector from the shear center to the midline segment ds. Consequently, the differential sectorial coordinate $d\omega$ serves as the basis for the warping displacement function, representing the geometric rate of change in longitudinal deformation across the section. The sectorial coordinate $\omega(s)$ is defined as twice the area swept by a position vector originating from the Shear Center as it moves along the midline of the cross-section.

Furthermore, $\Omega(s_1)$ also means the mean value of Ω over the cross-section area, in other words, “Sectorial Centroid”,

$$\Omega(s_1) \equiv \overline{\Omega} = \frac{1}{A}\int \quad t(s)\Omega(s)ds \quad (20)$$

The value $\Omega(s_1)$ represents the mean sectorial area, effectively acting as the Sectorial Centroid. Determining this value is a critical condition for locating the warping point s_1. This ensures that the resulting twisting deformation induces only warping displacement without generating a net axial lengthening or shortening of the member. Consequently, the first orthogonality condition is satisfied,

$$\int_A \omega(s)dA = 0 \quad (21)$$

One of the most practical applications of sectorial area is identifying “Shear Center”. Vlasov proved that the shear center is the point where the first sectorial moment of area equals zero (see Eq. 21). By developing a method based on "sweeping" the section, he provided a universal algorithm to find the exact point where a load must be applied to avoid twisting, regardless of how complex the profile geometry is.

2.2.1. Saint-Venant Theory

The tangential displacement v_s at any point along the midline defined by "natural coordinate" *s* is the product of the rotation angle $\theta(x)$ and Sectorial Radius $R(s,n)$ the perpendicular distance from the rotation center to the tangent at that point:

$$v_s(x,s) = u_y \frac{dy}{ds} + u_z \frac{dz}{ds} \tag{22}$$

$$v_s(x,s) = (-\theta(x)z)\frac{dy}{ds} + (\theta(x)y)\frac{dz}{ds} \tag{23}$$

$$v_s(x,s) = \theta(x)\underbrace{\left(y\frac{dz}{ds} - z\frac{dy}{ds}\right)}_{R(s)} \tag{24}$$

It is also defined as:

$$v_s(x,s) = \frac{d\Omega(s)}{ds} \cdot \theta(x) \tag{25}$$

In thin-walled members, the shear strain γ_{xs} in the plane of the wall along the natural coordinate *s* and longitudinal axis *x* is defined as the sum of the partial derivatives of the displacements. Vlassov's theory assumes that the shear strain on the middle surface of the thin-walled profile is negligible. Setting $\gamma_{xs} = 0$:

$$\gamma_{xs} = \frac{\partial u_x}{\partial s} + \frac{\partial v_s}{\partial x} = 0 \tag{26}$$

$$\frac{\partial u_x}{\partial s} = -\frac{\partial v_s}{\partial x} \tag{27}$$

If Eq. 24 is introduced into the Eq. 25,

$$\frac{\partial u_x}{\partial s} = -R(s) \cdot \frac{d\theta(x)}{dx} = -R(s) \cdot \theta'(x) \tag{28}$$

$$u_x(x,s) = -\theta'(x) \int R(s)\ ds \tag{29}$$

$$u_x(x,s) = -\omega(s) \cdot \theta'(x) \tag{30}$$

To find the shear strain at any point at a distance *n* from the midline, we consider the effective radius *R(s)+n*, Eq. 19 is introduced into the Eq. 28,

$$\frac{\partial u_x}{\partial s} = -\frac{d\omega}{ds}\theta'(z) \tag{31}$$

If Eq. 31 is introduced into the Eq. 26,

$$\gamma_{xs} = (R(s,n) + n)\theta' - \left(\frac{d\omega}{ds}\right)\theta' \tag{32}$$

If Eq. 19 is introduced into the Eq. 32,

$$\gamma_{xs} = \big(R(s,n) + n - R(s,n)\big)\theta' = n \cdot \theta' \tag{33}$$

Considering both Eq. 33 and the analogy of Hooke Theory $\tau = G \cdot \gamma$,

$$\tau_{sv} = G.\gamma_{xs} = G \cdot n \cdot \theta' \tag{34}$$

This stress varies linearly through the wall thickness *t* between *-t/2* and *t/2*. When we take the integral over the cross-sectional area to calculate the moment force generated by these stresses. In St. Venant torsion, the moment force is generated by the 'twisting' of the wall itself about its own centroid. Consequently, while the lever arm *n*

represents the distance from the mid-line (centerline) of the wall, the sectorial radius *R* is computed from the shear center.

$$M_{sv} = \int_A \tau \cdot n \, dA = \int_s \left(\int_{-t/2}^{t/2} (G \cdot n \cdot \theta') \cdot n \, dn \right) ds \tag{35}$$

$$M_{sv} = G\theta' \int_s \left[\frac{n^3}{3} \right]_{-t/2}^{t/2} ds = G\theta' \int_s \frac{t^3}{12} ds \tag{36}$$

$$M_{sv} = G\theta' \sum \left(\frac{1}{3} b_i t_i^3 \right) = G \cdot J \cdot \theta' \tag{37}$$

If it is considered Eq. 35, it is seen that the stress is zero at the mid-line (or middle axis) of the wall where *n=0*. As the distance from the center increases (as *n* increases), the stress increases.

2.2.2. Vlasov Theory

Just as in the analogy of normal and shear stresses σ and τ, σ_ω and τ_ω represent the warping normal stress and warping shear stress, respectively. While the expression ($\tau_\omega \, t$) and ($\sigma_\omega \, t$) denotes the Warping shear force per unit length (warping shear flow) and Warping normal force per unit length, respectively

$$\sum F_x = 0 \tag{38}$$

$$\sum F_x = \underbrace{F_{x2} - F_{x1}}_{\text{Normal Frorce}} + \underbrace{F_{s2} - F_{s1}}_{\text{Shear Froce}} = 0 \tag{39}$$

$$\left[\left(\sigma_\omega t + \frac{\partial(\sigma_\omega t)}{\partial x} dx \right) ds - (\sigma_\omega t) ds \right] + \left[\left(\tau_\omega t + \frac{\partial(\tau_\omega t)}{\partial s} ds \right) dx - (\tau_\omega t) dx \right] = 0 \tag{40}$$

$$\frac{\partial(\sigma_\omega t)}{\partial x} dx \cdot ds + \frac{\partial(\tau_\omega t)}{\partial s} ds \cdot dx = 0 \tag{41}$$

$$\frac{\partial(\sigma_\omega t)}{\partial x} + \frac{\partial(\tau_\omega t)}{\partial s} = 0 \tag{42}$$

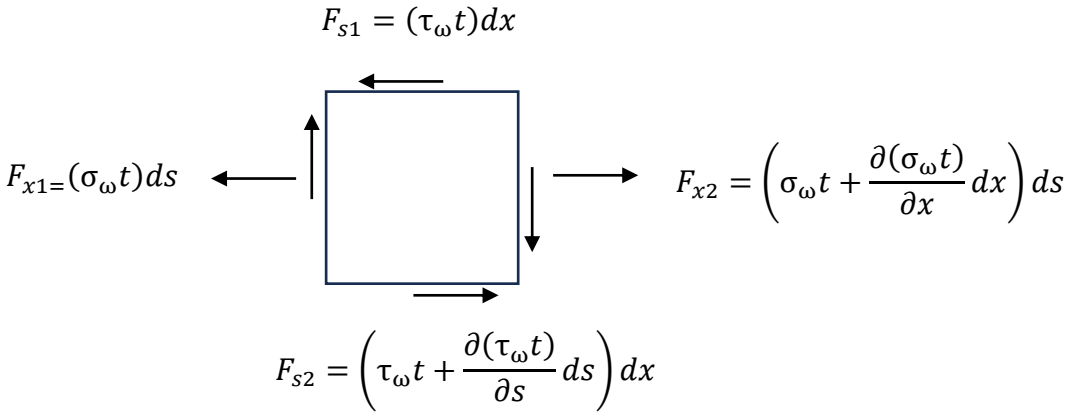


Figure 2. Equilibrium of Forces on A Differential Cross-sections

Just as in the bending analogy (reminding the moment force from the normal stresses $M = \int \sigma \cdot y \, dA$ with respect to neutral axis) and considering the derivation of Eq.4, warping torsional moment from normal stress σ with respect to shear center:

$$M_\omega = \int \tau_\omega \cdot \mathrm{R}(s) \cdot t \, ds \tag{43}$$

In Eq.43, $d\omega = R(s) ds$ idi,

$$M_\omega = \int_s (t\tau_\omega) \, d\omega \tag{44}$$

According to the partial integration rule ($\int u\ dv = [u \cdot v] - \int v\ du$),

$$M_\omega = [(t\tau_\omega) \cdot \omega]_{s_0}^{s_1} - \int_s \omega \cdot \frac{\partial(t\tau_\omega)}{\partial s}\ ds \tag{45}$$

Since there is no material beyond the free ends of the profile (e.g., the tips of an I-beam flange), there is no medium to support a shear force. Therefore, the shear flow must start and end at zero at these boundaries. For open cross-sections, the warping shear stress is zero at the endpoints (free edges) of the section ($\tau_\omega=0$). Consequently, the boundary values within the integration terms vanish,

$$M_\omega = -\int_s \omega \cdot \frac{\partial(t\tau_\omega)}{\partial s}\ ds \tag{46}$$

$$M_\omega = -\int_s \omega \cdot \left(-\frac{\partial(t\sigma_\omega)}{\partial x}\right)\ ds \tag{47}$$

$$M_\omega = \frac{d}{dx}\int_s \sigma_\omega \cdot \omega(s) \cdot t(s).\ ds \tag{48}$$

In Vlasov theory, the definition of "Bi-moment" B,

$$B = \int_A \sigma_\omega \cdot \omega(s)\ dA = \int_A \sigma_\omega \cdot \omega(s) \cdot t(s)\ ds \tag{49}$$

$$B = \int_A [-E\theta''(x)\omega(s)] \cdot \omega(s)\ dA \tag{50}$$

$$B = -E\theta''(x)\int_A \omega^2(s)\ dA \tag{51}$$

If Eq. 51 is introduced into Eq. 48,

$$M_\omega = \frac{dB}{dx} \tag{52}$$

Moreover, In Eq.51, it is possible to obtain "Sectorial Torsional Inertia Moment" I_ω or "warping constant" K_w as,

$$K_\omega = \int_A \omega^2(s)\ dA \tag{53}$$

If Eq.53 is introduced into Eq. 51,

$$B = -E\theta''(x) \cdot K_\omega \tag{54}$$

Also, Considering Eq. 49, it is possible to define "sectorial static moment" S_w as,

$$S_\omega(s) = \int_0^s \omega(s) \cdot t(s) ds \tag{55}$$

$$M_\omega = \frac{dB}{dx} = -E\theta'''(x) \cdot K_\omega \tag{56}$$

Just as in the bending analogy (reminding the normal stress $\sigma=E\varepsilon$, the warping normal stress,

$$\sigma_\omega = E\frac{\partial u}{\partial x} = -E\theta''(x)\omega(s) \tag{57}$$

If Eq. 54 is introduced into Eq. 57,

$$\sigma_\omega = \frac{B}{K_\omega}\ \omega(s) \tag{58}$$

Moreover, warping shear force per unit length (warping shear flow),

$$T_\omega = t\tau_\omega = -\int \frac{\partial(t\sigma_\omega)}{\partial x}\ ds \tag{59}$$

If Eq.55 and Eq.58 is introduced into Eq. 59,

$$\tau_\omega = -\frac{dB/dx}{K_\omega}\underbrace{\int_0^s \omega \cdot t\, ds}_{S_\omega(s)} \tag{60}$$

$$\tau_\omega = -\frac{M_\omega \cdot S_\omega(s)}{K_\omega \cdot t} \tag{61}$$

In classical bending, the shear stress τ is proportional to $Q(s)$ (reminding $\tau(s) = \frac{V \cdot Q(s)}{I \cdot t(s)}$). First Moment of Area $Q(s)$ indicates how "asymmetrically" the area of a section is distributed relative to the Neutral Axis. It determines the magnitude of the transverse shear stress required to maintain equilibrium during bending. Sectorial Static Moment $S_\omega(s)$ characterizes the "asymmetry" of the Sectorial Area distribution relative to the warping center. It serves as the distribution function for warping-induced shear stresses τ_ω resulting from the warping torsional moment M_ω.

Moreover, it is noted for the "sectorial static moment" S_w
For $S_1 = 0$,

$$S_\omega(s_1) = \int_0^0 \omega(s)t(s)ds = 0 \tag{62}$$

For S_2 = *the width of Flange or web,*

Considering Eq,58, the axial force,

$$\int_{s_1}^{s_2} \sigma_\omega t ds \quad = \frac{B}{K_\omega}\int_{s_1}^{s_2} t\,\omega(s)ds = \frac{B}{K_\omega}S_\omega(s_2) = 0 \tag{63}$$

Therefore,

$$S_\omega(s_2) = 0 \tag{64}$$

In an open cross-section, to maintain the equilibrium of the total bi-moment generated by the longitudinal normal stresses σ_ω, the total sectorial static moment must vanish $S_\omega = 0$ when reaching the end of the section contour

Moreover, if there is no externally applied tangential shear force at the free edge s_2, the warping shear stress τ_ω must be zero (that is, $\tau_\omega(s_2) = 0$). Thus,

$$\frac{B \cdot S_\omega(s_2)}{I_\omega \cdot t(s_2)} = 0 \tag{65}$$

Therefore,

$$S_\omega(s_2) = 0 \tag{66}$$

2.2.3. The General Vlasov Differential Equation for Non-uniform Torsion

The thin-walled members, the total torque is resisted by two mechanisms: St. Venant (uniform) torsion and Warping (non-uniform) torsion. Thus, the differentiation in the sum of St. Venant (uniform) and Warping (non-uniform) torsional moment have to be equal to "0". In this regard, considering the Eq. 56 and Eq.37, the equilibrium based on the Vlasov differential equation for non-uniform torsion is expressed as:

$$EI_\omega \theta^{iv}(x) - GJ\theta''(x) = m(x) \tag{67}$$

Thus, this general equation of Vlasov is solved depending on the boundary condition.

2.2.4. The Brief Introduction to Basic Principles of "ElasticBeamWarping3d" utilized in OpenseesPy

In Finite Element Analysis, the goal is to transform a continuous differential equation into a discrete matrix equation. The "bridge" used to cross this gap is the Shape Function. The governing equation for Vlasov torsion is a 4th-order differential equation. To solve this using the Finite Element Method, the interpolation function used to

guess the torsional angle between two nodes must be "mathematically rich" enough to satisfy the boundary conditions of both the torsional angle and the derivative of torsional angle (warping). Due to having a 4th-order equation, a linear or quadratic guess is insufficient. A cubic polynomial is the lowest degree that allows us to calculate the necessary derivatives for warping energy without the math "disappearing" to zero. Furthermore, Standard shape functions (like Lagrange) only ensure that the torsional angle is the same where two elements meet. Hermite polynomials ensure that both the torsional angle and the derivative of torsional angle (warping) are continuous. Hermite functions ensure that the beam warps smoothly across elements without "cracking". Thus, firstly, the torsional angle at any point along the beam is assumed as a combination of 4 Hermite functions multiplied by the nodal value. Then, the energy equation is guessed. The total internal energy of the beam consists of two parts: Warping Energy related to the second derivative of torsional angle and Saint-Venant Torsion Energy related to the first derivative of torsional angle. The energy integration is resulted with the stiffens matrix coefficients. In most FEA applications (like standard bending), shape functions are just an "approximation." However, for the 4th-order torsion-warping problem, the cubic polynomial is mathematically equivalent to the exact homogeneous solution of the differential equation. This result is validated by the performance tests in the following parts.

3. Application: A Cantilever Beam with Symmetric, Semi-symmetric and Asymmetric type cross-sections

In this specific case study, a steel profile beam with Symmetric, Semi-symmetric and Asymmetric cross-sections is analyzed under a torque generated by a 500 N point load in the end of length of 6000 mm. This application provides a robust analytical framework for the torsional analysis of thin-walled open sections, including I-profile (IPE 300), U-channel (UPN 200), and Z-section (ZNP 160).

The comparative analysis between the dedicated MATLAB analytical solver and the OpenSeesPy numerical model reveals critical insights into the non-uniform torsional behavior of thin-walled members. The initial validation phase demonstrated a mathematically perfect correlation (100% agreement) between the two platforms across all evaluated cross-sections. This exact equivalence is not merely coincidental; it is a direct consequence of the underlying mathematical formulations. As discussed in Section 2.2.4, the general Vlasov equation for non-uniform torsion is a fourth-order linear differential equation. The elasticBeamColumnWarping3d element in OpenSeesPy utilizes cubic Hermitian shape functions to interpolate the torsional angle across the element nodes. Because cubic polynomials are mathematically capable of representing the exact homogeneous solution of this fourth-order equation, the finite element formulation inherently avoids standard discretization errors, converging identically to the exact closed-form analytical solution provided by the MATLAB solver. This confirms that the finite element implementation strictly and accurately utilizes the Vlasov stiffness matrix to map the fundamental warping degrees of freedom.

Beyond numerical validation, the distribution of the torsional rotation angle (θ) and the bi-moment (B) across the beam length physically illustrates the distinct kinematic behaviors of symmetric, semi-symmetric, and asymmetric cross-sections under restrained warping conditions:

- Symmetric I-Profile (IPE 300): For doubly symmetric sections, the shear center perfectly coincides with the geometric centroid (see Figure 2a). The warping resistance is provided symmetrically by the differential lateral bending of the top and bottom flanges. As seen in Figure 3, the bi-moment distribution exhibits a steep gradient at the fixed support—where the warping derivative (θ') is strictly enforced to zero—and exponentially decays toward the free end. The pure symmetry ensures that torsional demands do not induce lateral or vertical bending, allowing the St. Venant and warping torsional mechanisms to act purely in parallel (see Figure 2b).
- Semi-symmetric U-Channel (UPN 200): In mono-symmetric sections, the shear center lies outside the cross-sectional envelope (see Figure 4a). Consequently, the sectorial area distribution relies almost entirely on the asymmetrical bending of the flanges, as the web lies on the primary axis of rotation and provides negligible warping resistance. Figure 5 illustrates how this spatial eccentricity alters the bi-moment distribution (see the deformed form in Figure 4b). The separation between the centroid and the shear center means that any torsional rotation inherently couples with transverse displacements, making the correct spatial mapping of the 7th-DOF in OpenSeesPy physically critical to capture the true structural response.
- Asymmetric Z-Profile (ZNP 160): Point-symmetric or asymmetric sections present the most complex sectorial kinematics. While the shear center aligns with the centroid, the principal bending axes are inclined, resulting in a highly irregular sectorial area (ω_s) distribution (see Figure 6a). As illustrated in Figure 7, the coupling of out-of-plane warping displacements becomes highly sensitive to the cross-sectional geometry (see the deformed form in Figure 6b).

Crucially, the evaluation of the ZNP 160 profile highlights a fundamental limitation in simplified engineering practices. Although standard industry tables provide estimated warping constants (I_ω) based on idealized flange contributions, they frequently fail to apply the rigorous sectorial area correction (normalization) relative to the exact shear center. The analytical MATLAB engine demonstrates that if the sectorial coordinate (ω_s) is not strictly orthogonalized against the cross-sectional area ($\int_A \omega_s dA = 0$), the kinematic formulation will artificially generate spurious longitudinal axial forces under pure torsion. In finite element environments, this lack of normalization leads to severe numerical instability or "locking" phenomena. The MATLAB solver performs this exact sectorial centroid normalization, proving that computing the mathematically "correct" base values is an absolute necessity for defining the 7-DOF boundary conditions accurately. Ultimately, the robust alignment between the platforms validates that the proposed analytical methodology acts as a vital, high-precision calibration tool for advanced structural engineering applications.

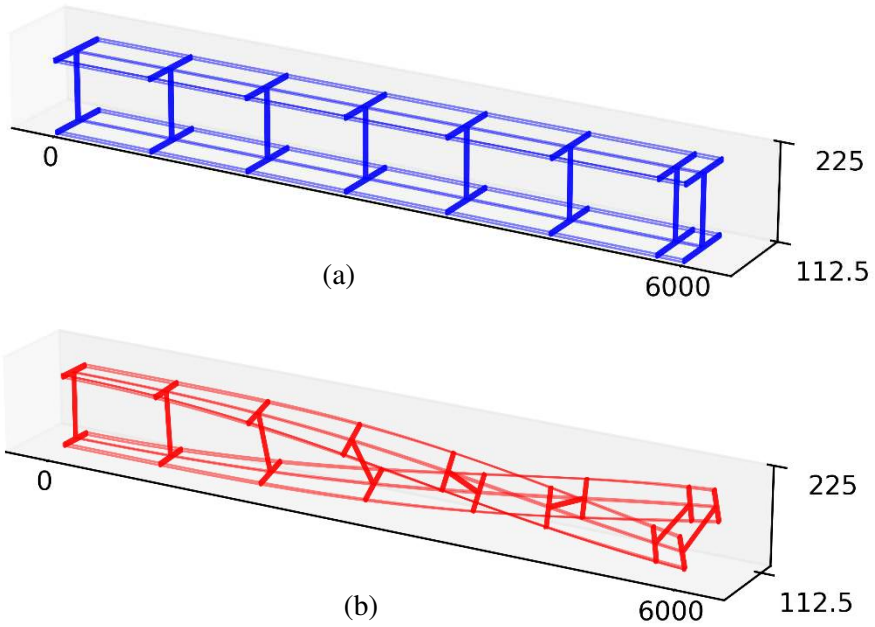


Figure 2. The Cantilever Beam with I-profile (IPE 300: Undeformed Form (a) and Deformed Form (b)

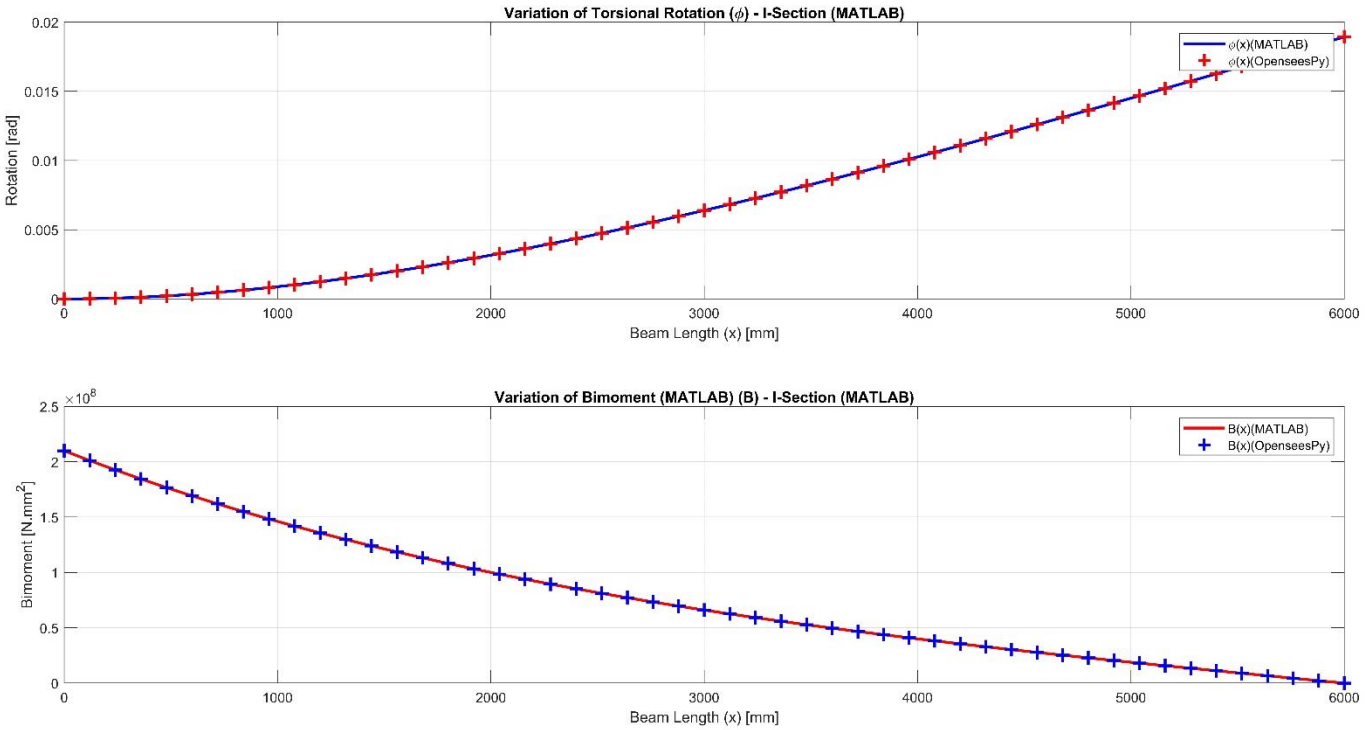


Figure 3. Torsional Rotation Angle and Bi-moment Variation throughout The Cantilever Beam with I-profile (IPE 300) obtained by MATLAB Solver and OpenSeesPy

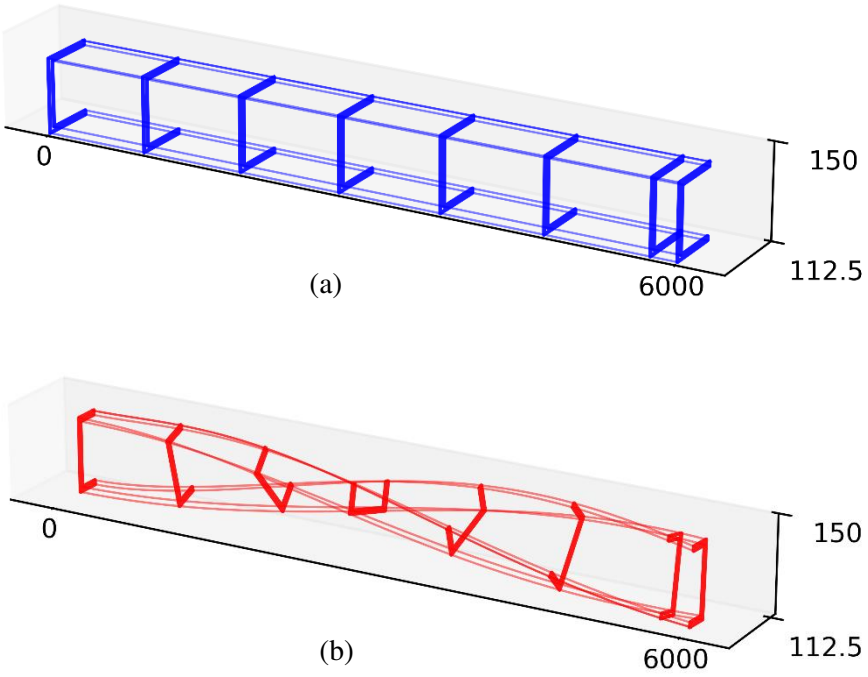


Figure 4. The Cantilever Beam with U-profile (UPN 200): Undeformed Form (a) and Deformed Form (b)

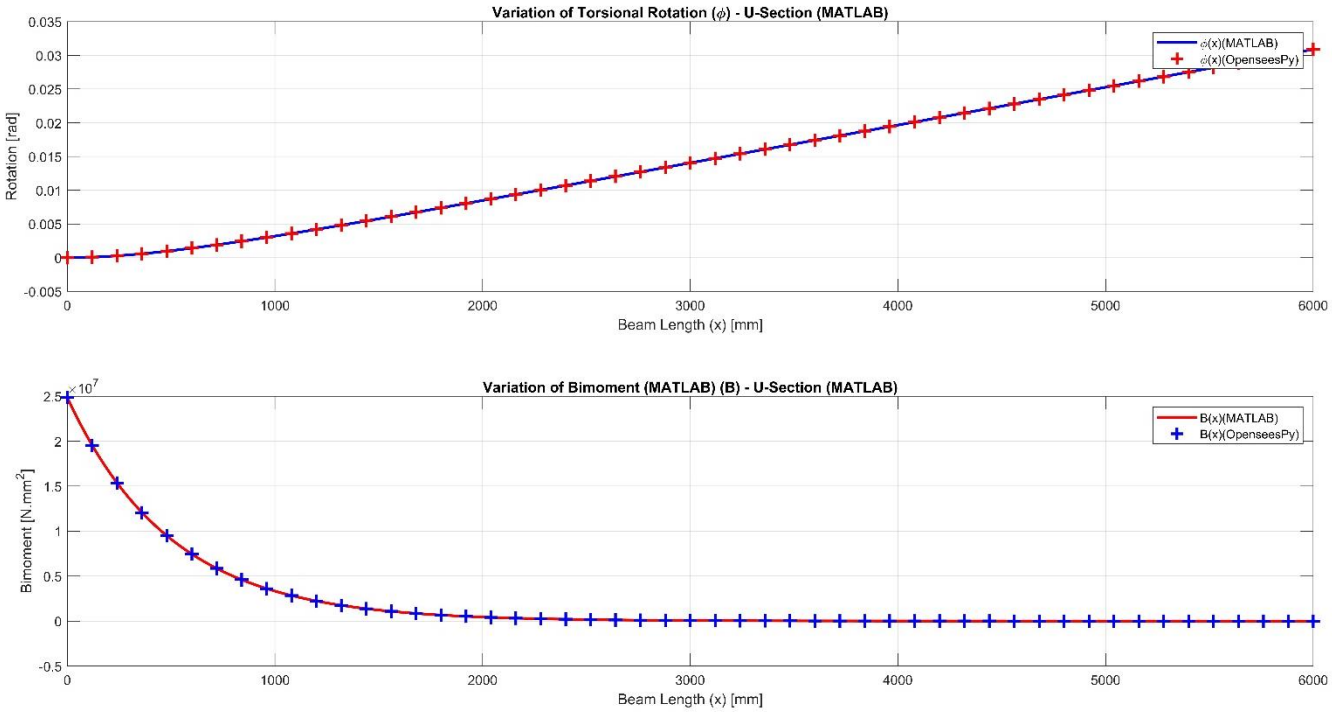


Figure 5. Torsional Rotation Angle and Bi-moment Variation throughout The Cantilever Beam with U-profile (UPN 200) obtained by MATLAB Solver and OpenSeesPy

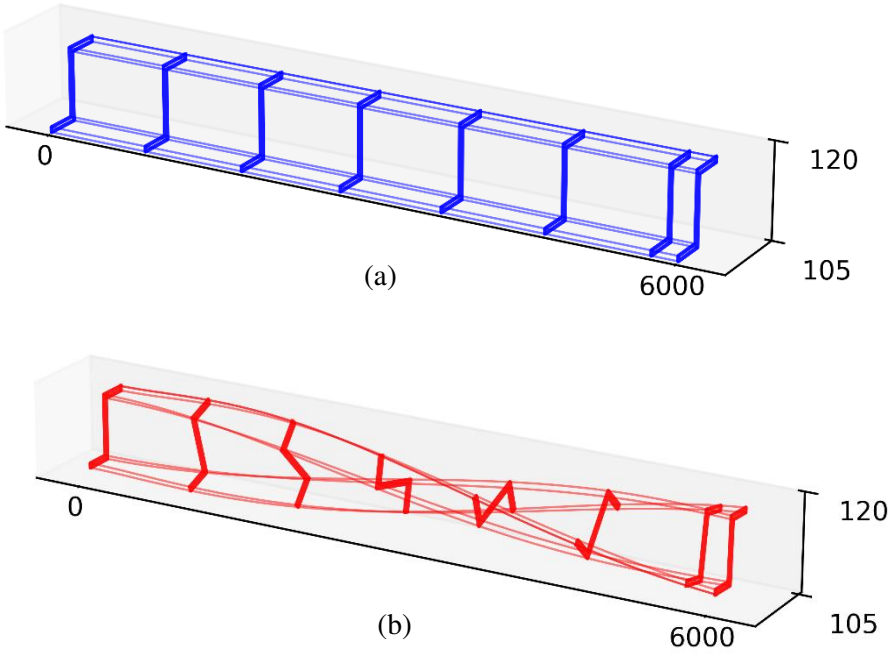


Figure 6. The Cantilever Beam with Z-profile (ZNP 160): Undeformed Form (a) and Deformed Form (b)

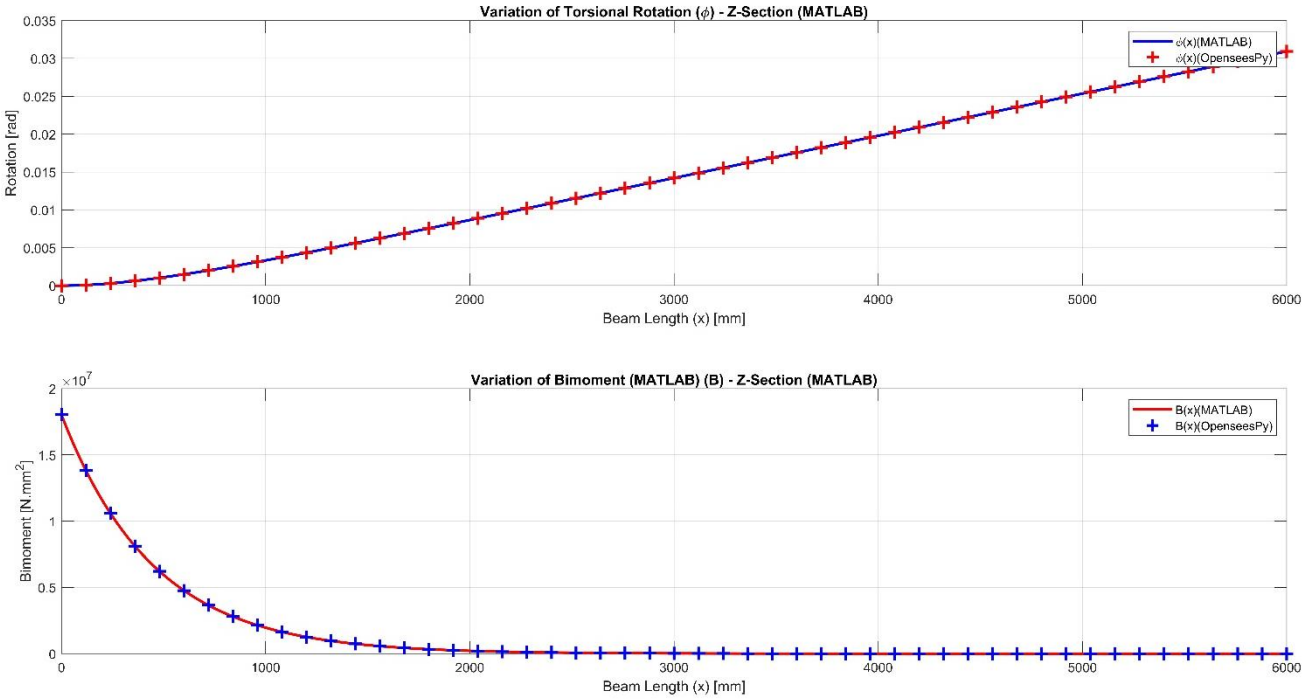


Figure 7. Torsional Rotation Angle and Bi-moment Variation throughout The Cantilever Beam with Z-profile (ZNP 160) obtained by MATLAB Solver and OpenSeesPy

4. Conclusion

This study successfully demonstrates a robust validation framework for the torsional analysis of thin-walled open sections by integrating Vlasov's Theory of Thin-Walled Beams into two independent computational platforms: a custom-coded MATLAB analytical solver and an OpenSeesPy numerical model. ***The source code of MATLAB analytical solver and input codes of OpenSeesPy numerical model are presented as a supplementary material for this study.***

The investigation achieved a 100% match (perfect correlation) between the MATLAB analytical solutions and the OpenSeesPy "ElasticBeamWarping3d" element results. This equivalence confirms that the finite element implementation correctly utilizes the Vlasov stiffness matrix and accurately maps the fundamental warping degrees of freedom across diverse geometries.

The MATLAB-based Precision Sectoral Analysis Engine highlighted the critical importance of sectorial area normalization relative to the shear center, particularly for asymmetric sections like the ZNP 160. While standard industry tables provide a reliable baseline for warping contributions, the custom analytical solver offers the mathematically "correct" values required for high-precision structural engineering by accounting for a real-world geometric nuance.

In summary, the consistency between the independent analytical and numerical platforms ensures a high degree of reliability for the elastic torsion and warping analysis of industrial structures. As a next study, the steel structural elements with not only "I" type cross-sectionals but also the other types will be evaluated for an elasto-plastic analysis considering the non-uniform torsional responses.

Data Availability

The source code of MATLAB analytical solver and input codes of OpenSeesPy numerical model are presented as a supplementary material for this study.

Author Contribution

The author confirms sole responsibility for the following: study conception and design, data collection, analysis and interpretation of results, and manuscript preparation

Conflict of Interest / Declaration of Competing Interest

The author declares that they have no known competing financial interests or personal relationships that could have appeared to influence the work reported in this paper

Funding Declaration

The author declares that there was no Funding which is utilized for this paper.

References

[1] Barré de Saint-Venant, A. J. C. (1855). Mémoire sur la torsion des prismes. Mémoires présentés par divers savants à l'Académie des Sciences, 14, 233-560.
[2] Vlasov VZ (1961) Thin-walled elastic beams. Israel Program for Scientific Translations, Jerusalem
[3] Timoshenko SP, Goodier JN (1970) Theory of elasticity, 3rd edn. McGraw-Hill, New York
[4] Benscoter SU (1954) A theory of torsion sections for thin-walled beams. J Appl Mech 21:32-34. https://doi.org/10.1115/1.4010795
[5] Kollbrunner CF, Basler K (1969) Torsion in structures. Springer-Verlag, Berlin
[6] Bažant ZP, El Nimeiri M (1973) Stiffness method for curved box girders at initial stress. J Struct Div 99:2115-2142. https://doi.org/10.1061/JSDEAG.0003618
[7] Yoo CH, Lee SC (2011) Stability of structures: principles and applications. Butterworth-Heinemann, Oxford
[8] Gjelsvik A (1981) The theory of thin walled bars. John Wiley & Sons, New York
[9] Trahair NS (1993) Flexural-torsional buckling of structures. CRC Press, Boca Raton
[10] Barsoum RS, Gallagher RH (1970) Finite element analysis of torsional and torsional-flexural stability. Int J Numer Meth Eng 2:335-352. https://doi.org/10.1002/nme.1620020304
[11] Mohri F, Azrar L, Potier-Ferry M (2001) Theoretical and numerical analysis of non-linear torsional–flexural buckling of thin-walled beam–columns. Int J Solids Struct 38:5285-5314. https://doi.org/10.1016/S0020-7683(00)00346-4.
[12] Burlon, A., et al. (2023). "Application and Experimental Validation of Seven-Degree-of-Freedom Beam Element for Girder Bridges during Deck Construction." Materials, 16.
[13] Kameshki, M., & Kazem, M. (2024). "Advanced non-uniform torsion analysis of thin-walled members using computational frameworks". Journal of Constructional Steel Research, 212, 108250.
[14] Denavit, M. D., & Hajjar, J. F. (2023). "A Displacement-Based Fiber Element to Simulate Interactive Lateral Torsional and Local Buckling in Steel Members". Journal of Structural Engineering (ASCE), 149(3), 04023005.
[15] McKenna G, Fenves GL, Scott MH (2000) Open system for earthquake engineering simulation. University of California, Berkeley. http://opensees.berkeley.edu. Accessed 19 March 2026
[16] Zhu M, McKenna F, Scott MH (2018) OpenSeesPy: Python library for the OpenSees finite element framework. SoftwareX 7:6-11. https://doi.org/10.1016/j.softx.2017.10.009Timoshenko, S. P., & Goodier, J. N. (1970). Theory of Elasticity (3rd ed.). New York: McGraw-Hill.
[17] Larsson R (2005) A course on computational solid mechanics. Division of Material and Computational Mechanics, Chalmers University of Technology, Gothenburg. http://www.chalmers.se. Accessed March 2026